Multiphoton Reduction of Eu^{3+} to Eu^{2+} in Methanol Using Intense, Short Pulses from a Ti:Sapphire Laser

Nobuaki Nakashima*

Department of Chemistry, Graduate School of Science, Osaka City University, 3-3-138 Sugimoto, Sumiyoshi, Osaka 558-8585, Japan

Shin-ichi Nakamura and Shuji Sakabe[†]

Department of Electromagnetic Energy Engineering, Osaka University, 2-1 Yamada-oka, Suita, Osaka 565-0871, Japan

Helmut Schillinger,[‡] **Yasushi Hamanaka,**[§] **and Chiyoe Yamanaka**

Institute for Laser Technology, 2-6 Yamada-oka, Suita, Osaka 565-0871, Japan

Mitsuhiro Kusaba

Department of Electrical Engineering and Electronics, Osaka Sangyo University, 3-1-1 Nakagaito, Daito, Osaka 574-8530, Japan

Nobuo Ishihara

Chemical Lab. Takasago Inst. Mitsubishi Heavy Industry Ltd., 2-1-1 Niihama, Arai, Takasago, Hyogo 676-0008, Japan

Yasukazu Izawa

Institute of Laser Engineering, Osaka University, 2-6 Yamada-oka, Suita, Osaka 565-0871, Japan

Received: October 22, 1998; In Final Form: March 11, 1999

Multiphoton reduction of Eu^{3+} to Eu^{2+} in methanol was induced by irradiation with the second harmonic (394 nm, 2 ps) of a Ti:sapphire laser. The conversion efficiencies were increased to 0.3 for short pulse excitation, as compared to on the order of 10^{-5} for a nanosecond dye laser pulse. It appears that a three-photon process pumps a deep charge-transfer state from which Eu^{3+} efficiently dissociates to Eu^{2+}. On the basis of the excitation spectra, the first intermediate state is the $^5L_6$ state, which is one of the f-electronic excited states. The Eu^{2+} concentration increased shot by shot and approached a plateau. The saturation behavior will be explained in terms of the back photooxidation of Eu^{2+} to Eu^{3+}.

1. Introduction

Lanthanide and actinide ions display line-like absorptions due to the inner f-shell transitions in the UV−vis regions. No photoredox reaction can be induced by single-photon excitation of the f-electronic transitions. In the vis−VUV regions, the lanthanide and actinide ions have charge-transfer (CT) bands,[1] in which charge separation can be induced by photoexcitation. Two-photon chemistry via the f-electronic transitions has been proposed by Donohue.[2] The first photon produces an f-electronic excited state and the subsequent photons pump a charge-transfer (CT) state. The first reported example of the above scheme is the oxidation of Sm^{2+} to Sm^{3+} in a BaClF crystal.[3] The $^5D_0 \leftarrow {}^7F_0$ or $^5D_1 \leftarrow {}^7F_0$ transitions of Sm^{2+} were induced with CW red dye lasers, and the second green photon ionizes Sm^{2+} to $Sm^{3+} + e$. The two-photon reduction of Eu^{3+} to Eu^{2+} in methanol was carried out by the present group.[4] This is the first reported example of the above scheme in solution. The excitation spectra are in agreement with the absorption spectra of the f-electronic transitions of Eu^{3+}, and we can therefore assume that the intermediates are the f-electronic excited states.

The efficiency of Eu^{3+} to Eu^{2+} in the two-photon reduction was as low as 10^{-5}, when the exciting laser was a dye laser with a pulse width of 20 ns. One major reason for the low yield is probably the short lifetime of the intermediate state. In this paper, the exciting pulse had subpicosecond and picosecond pulse widths instead of a nanosecond laser pulse. It has been shown that the efficiency of the reduction increases dramatically by several orders of magnitude when these short pulse widths are used.[5] Short, intense excitation overcomes the short lifetime of the intermediate and results in the pumping of a labile CT state. The nature of the second and third photon states are not very clear; however, we call them CT states in this paper because charge separation eventually takes place from the states. To explain the saturation effect and the high efficiency reported

[†] Another affliation: Institute of Laser Engineering, Osaka University, 2-6 Yamada-oka, Suita, Osaka 565-0871, Japan.

[‡] Present address: IOQ, PATF Friedrich-Schiller-Univ., Max-Wien-Platz 1, 07741 Jena, Germany.

[§] Present address: Dept. Applied Physics, Nagoya Univ., Chikusa Nagoya 464-0814, Japan.

10.1021/jp984120t CCC: $18.00
Published on Web 04/30/1999

here, the back-reaction and the role of the third photon must be considered. The back-reaction is a photooxidation of Eu^{2+} to Eu^{3+}. Two-color and two-photon reduction by nanosecond dye lasers has been preliminary reported[6] and the related data are added.

2. Experimental Section

Light pulses were delivered from a chirped-pulse amplified Ti:sapphire laser system.[7] The laser system was capable of producing an output energy of 180 mJ in a short pulse width of 100 fs with a repetition rate of 10 Hz and at a central wavelength of 790 nm. The laser energy of the second harmonic was less than 0.79 mJ per pulse. The pulse widths were monitored with a single-shot autocorrelator[7] for the fundamental wavelength. The major experiments were carried out with 2 ps pulses. The laser beam was focused with a dielectric mirror with a 150 mm focal length, and the spot size at the cell position was determined to be 1.6×10^{-3} cm^2 using a CCD camera. The maximum photon intensity after corrections for optical losses was estimated to be 0.48 J cm^{-2} or 2.5×10^{11} W cm^{-2}. The multiphoton absorption loss by the quartz window was low, but optical damage was occasionally seen after 10000-shot irradiation at the highest energy. The shortest pulse was 0.35 ps, which was estimated from a 0.2 ps pulse of the fundamental pulse to be elongated due to the group velocity mismatch in a BBO crystal of 1 mm thick for second harmonic generation. Some nonlinear phenomena were induced by focusing a 0.35 ps pulse with 0.015 mJ energy to a spot size of 1.1×10^{-2} cm^2. White continuum generation and induced Raman scattering were observed from pure methanol. These phenomena completely disappeared when a sample containing Eu^{3+} was replaced.

To pump the $^5L_6 \leftarrow {}^7F_0$ transition of Eu^{3+} in methanol solution, the second harmonic at 394.3 nm was generated by a BBO crystal; therefore, the central wavelength of the laser was tuned to 789 nm. The excitation wavelength at 394.3 nm was determined so as to give the maximum luminescence intensity at 618 nm (the $^5D_0 \rightarrow {}^7F_2$ transition) of Eu^{3+} ion. The spectral width at the fundamental wavelength was measured to be 7.5 nm as full width at half-maximum and the second harmonic was ca. 3.4 nm.

The cell size was 0.2 (width) $\times$ 0.4 (depth) $\times$ 20 mm (height) with a vacuum cock. $EuCl_3 \cdot 6H_2O$ (Aldrich) of stated purity of 99.9% was dissolved in 0.03 cm^3 of methanol (Dotite, Luminasol) with 0.345 M Eu^{3+} ion. The solution was degassed to avoid oxidizing Eu^{2+} with dissolved oxygen. The Eu^{2+} concentration after laser irradiation was determined by its fluorescence intensity. A calibration curve between the concentration and its fluorescence intensity was made. A Hitati F-4500 fluorophotometer was used to measure Eu^{2+} fluorescence with a typical slit width of 10 nm.

After the solution was irradiated for a number of shots, the Eu^{2+} fluorescence was measured to determine the concentration. The fluorescence measurement took about 10 min., and the next cycle of irradiation and measurement was then started.

For the two-color multiphoton experiments with 20 ns pulses, two Lambda Physik FL 3002 dye lasers were used. Those were pumped by Lambda Physik EMG 201MSC and LPX 100 excimer lasers. The sample was irradiated at 180° from different directions. The two beams were carefully adjusted in a collinear axis. The oscillation delay between the two lasers was controlled within a jitter of just a few nanoseconds using a DG535 (Stanford Research Systems) pulse generator. Other details of the experiments with the nanosecond lasers are described elsewhere.[4]

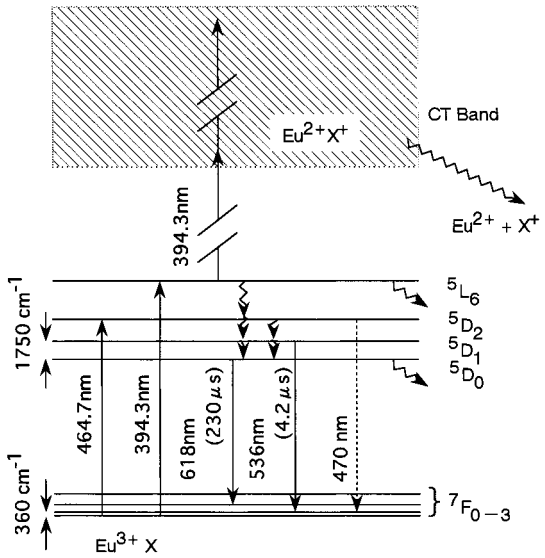

Figure 1. Scheme of the multiphoton reduction of Eu^{3+} to Eu^{2+} for $EuCl_3$ in methanol. Phototransitions are indicated by an arrow with a solid line and nonradiative transitions by a ripple line. The first step of the multiphoton reduction is the f′ ← f transition of $^5L_6 \leftarrow {}^7F_0$ or $^5D_2 \leftarrow {}^7F_0$. The shaded area is a CT band at a wavelength shorter than 350 nm. The excitation to the CT band causes the dissociation to Eu^{2+}. The absorption wavelengths to $^5L_6$ and $^5D_2$ levels[4] and emission lines with lifetimes[12,13] and energy gaps (Eu^{3+} (aq))[10] are taken from the literature.

The fluorescence lifetimes were measured with a photon-counting fluorometer. The excitation light source was the second harmonic of a picosecond dye laser or a Ti:sapphire laser, and the detector was R3809 (Hamamatsu Photonics). The total time resolution was 50 ps. $EuCl_2$ was synthesized according to the procedure in the literature.[8] Anhydrous $EuCl_3$ was kept at 1000 K for 2 h with mixed gases of hydrogen, nitrogen, and hydrogen chloride. The concentration of Eu^{2+} ion was determined by its known molar extinction coefficient.[9]

3. Results

3.1 Spectroscopic and Dynamical Properties of $EuCl_3$ and $EuCl_2$. Figure 1 shows a scheme of the multiphoton reduction of Eu^{3+} to Eu^{2+}. The related energy levels of Eu^{3+} ion are taken from literature.[10−13] Phototransitions (indicated by an arrow with a solid line) and nonradiative transitions (by a ripple line) are shown. The first step of the multiphoton reduction is an excitation of the f-electronic transition either of $^5L_6 \leftarrow {}^7F_0$ or $^5D_2 \leftarrow {}^7F_0$. $EuCl_3$ solution shows CT absorption bands in the wavelength region shorter than 350 nm.[11] One of these bands appears at 270 nm with a tail to 350 nm and is due to CT between Eu^{3+} and Cl^- and the other appears at 230 nm due to CT between Eu^{3+} and methanol. The direct excitation of the CT bands induces the reduction of Eu^{3+} to Eu^{2+}. The luminescence lifetime of the $^5D_0$ state is 230 μs for $Eu(ClO_4)_3$ in methanol and that of the $^5D_1$ state is 4.2 μs for $EuCl_3$ in methanol.[12,13] The lifetimes under the present conditions were 100 μs for the $^5D_0$ state and 3.4 μs for the $^5D_1$ state and are in fair agreement with the above. There has been no clear information on the lifetimes in solution for the mulutiphoton-active $^5L_6$ and $^5D_2$ states in the literature.[14] The luminescence rise and decay of $^5D_1 \rightarrow {}^7F_1$, 536 nm was observed by exciting the transition of $^5L_6 \leftarrow {}^7F_0$, 394.3 nm. No rise time was detected that was slower than the 50 ps response time. The results indicate that the lifetime of the $^5L_6$ state is shorter than 50 ps. The luminescence at 470 nm, where $^5D_2 \rightarrow {}^7F_1$ luminescence should

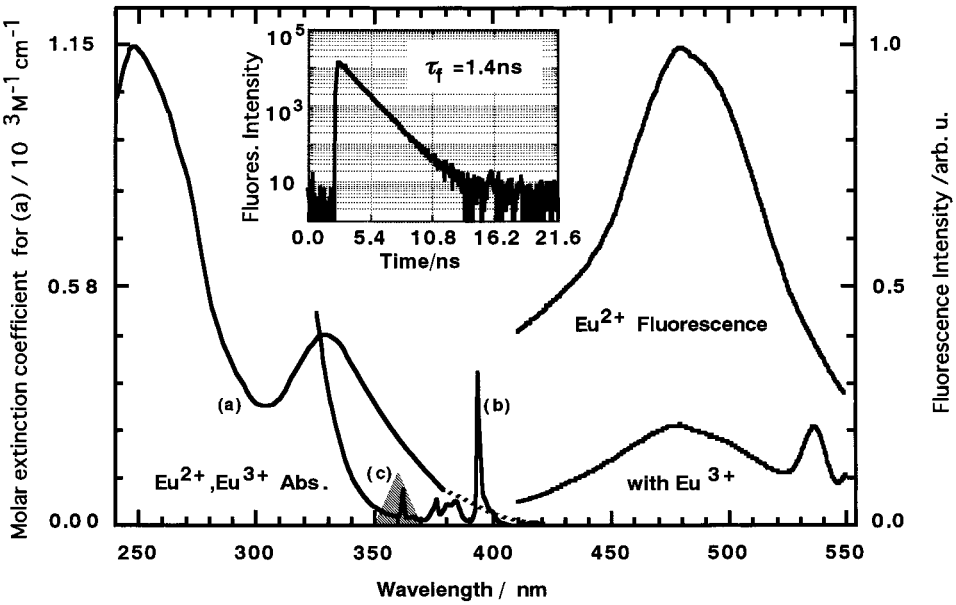

Figure 2. Absorption spectrum of $EuCl_2$ in methanol (left, part a (ref 8) and a dotted line added by this work) with molar extinction coefficients. A fluorescence decay of $EuCl_2$ 1×10^{-3} M in degassed solution (upper-middle) is measured by the photon-counting method with excitation at 290 nm. The fluorescence spectra (right) are from $EuCl_2$ 2.6×10^{-3} M solution (upper one) and from a 2.6×10^{-3} M $EuCl_2$ solution containing 0.345 M of $EuCl_3$ (lower one). Spectrum b is the absorption profile of $EuCl_3$ in methanol, having the molar extinction coefficient of 2.9 M^{-1} cm^{-1} at the peak of 394.3 nm. The shaded area c indicates the slit width of a monitoring light.

be, was measured. The weak luminescence showed a lifetime of 320 ps and may have been due to the decay of the $^5D_2$ state. It is true that the relaxation processes of the $^5L_6$ and $^5D_2$ states to the low-energy levels are rapid and efficient.

The spectroscopic properties of $EuCl_2$ in methanol are shown in Figure 2. The majority of the absorption spectrum and the molar extinction coefficients are taken from the literature,[9] and the spectrum is indicated by part a. The absorption of Eu^{2+} ion is attributed to the 5d ← 4f transition. The spectrum indicated by a dotted line was added and the scale was adjusted to the reference spectrum at 380 nm. The molar extinction coefficient at 394.3 nm was estimated to be 40 M^{-1} cm^{-1} and the same value has been reported for $EuCl_2$ in water.[15] The long wavelength side of the spectrum is important for our discussion. The fluorescence was broad peaked around 480 nm. A linear relationship between the fluorescence intensity and the Eu^{2+} concentration was experimentally obtained and used for determining the Eu^{2+} concentration. One of the important findings is that Eu^{2+} fluorescence is quenched by the Eu^{3+} ion. The fluorescence intensity in the presence of 0.345 M $EuCl_3$ diminished to 19% of that of the $EuCl_3$ free solution. The diminishment in intensity is reasonable because the absorption spectra of Eu^{3+} ion overlaps with the emission spectra of Eu^{2+}; for example, the transition at 464.7 nm ($^5D_2$ ← $^7F_0$) is in the region of Eu^{2+} fluorescence. The high concentration of the Cl^- ion could be the cause of the fluorescence quenching. The upper, middle figure is a decay curve of the fluorescence of 1×10^{-3} M $EuCl_2$ in degassed solution. The fluorescence lifetime was measured to be 1.4 ns using the photon-counting method, although a lifetime of 20 ns was reported.[9] The new value of 1.4 ns gives a quenching rate constant of 0.85×10^{10} M^{-1} s^{-1}, which is close to the diffusional rate constant of 1.2×10^{10} M^{-1} s^{-1} in methanol. The reasonable radiative rate constant is derived to be 2.9×10^5 s^{-1} in methanol from the lifetime and the fluorescence quantum yield[9] of 0.0004.

3.2. Eu^{2+} Formation by Laser Irradiation of $EuCl_3$ Solution. The luminescence color of an irradiated sample showed pink in the beginning of the experiments, and it then turned whitish. In fact, the initial color is due to the emission

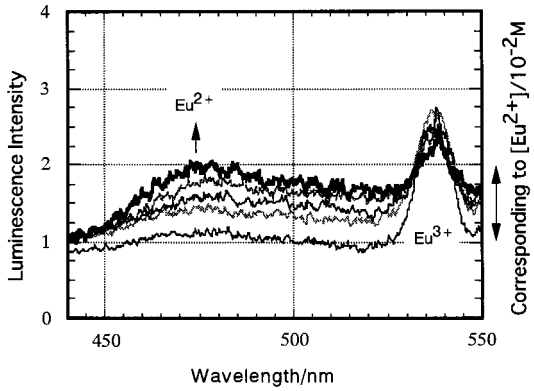

Figure 3. Luminescence after irradiating $EuCl_3$ solution with 0.79 mJ per pulse for 2 ps. The laser shot numbers were 0, 1000, 2000, 5000, and 10000 shots from the bottom spectrum to the top. The Eu^{2+} fluorescence around 480 nm increased irradiating laser pulses. The peak at 536 nm is assigned to the $^5D_2$ → $^7F_0$ luminescence of Eu^{3+}.

of Eu^{3+} around 618 nm. The whitish color after some laser shots indicates that the blue fluorescence by Eu^{2+} mixes with the pink Eu^{3+} luminescence. In Figure 3 it can be seen that the Eu^{2+} fluorescence around 480 nm increases by irradiating the $EuCl_3$ solution with 2 ps laser pulses with 0.79 mJ per pulse. The laser shot numbers were 0, 1000, 2000, 5000, and 10000 shots from the bottom spectrum to the top, respectively. The Eu^{2+} concentration after 10000-shot irradiation reached 8.4×10^{-3} M; in other words, 3% of the Eu^{3+} ions were converted to Eu^{2+}. The peak at 536 nm is assigned to the $^5D_2$ → $^7F_0$ luminescence of Eu^{3+}. The luminescence intensity of Eu^{3+} decreased with increases in the Eu^{2+} fluorescence intensity. An irradiated sample contains Eu^{2+} and Eu^{3+} ions. The absorption spectrum of Eu^{2+} is broad, while that of Eu^{3+} shows some structures and has a peak at 362 nm due to the Eu^{3+} transition of $^5D_4$ ← $^7F_0$ as seen in Figure 2c. The Eu^{2+} as well as Eu^{3+} ions absorb a monitoring light of Eu^{2+} with a central wavelength of 360 nm and a width of 10 nm. Therefore, the higher the concentration of Eu^{2+}, the lower the absorption intensity of Eu^{3+} relative to that of Eu^{2+} in the 10 nm. In Figure 4, the fluorescence

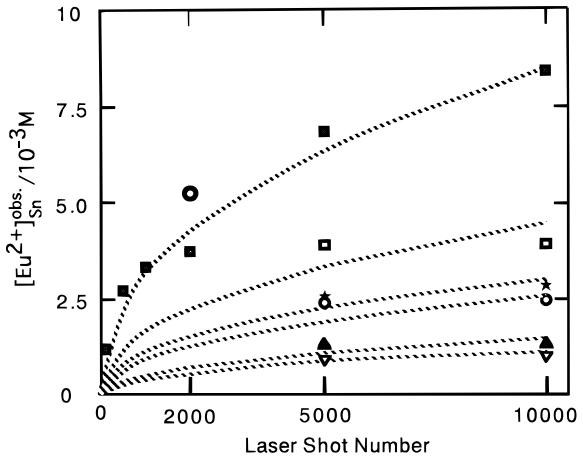

Figure 4. Production of Eu^{2+} vs laser shot number. Irradiation of $EuCl_3$ solution with 2 ps laser pulses. Laser energy per pulse: 0.79 mJ (■); 0.69 mJ (□); 0.60 mJ (★); 0.50 mJ (○); 0.41 mJ (▲); 0.31 mJ (▽). The broken lines are simulation curves taking into account the back reaction. The open large circle (◯) indicates the use of a moving cell with a pulse energy of 0.5 mJ.

intensities of Eu^{2+} are plotted vs the laser shot numbers at several different laser energies. The Eu^{2+} concentration became saturated as the number of laser-shots increased. This figure includes simulation curves (indicated by broken lines) in which the back-reaction is taken into account. (See the next section.)

One important observation is that a high concentration of Eu^{2+} was detected if a moving cell was used. This is indicated by a large circle at 2000 shot in Figure 4. The cell moved smoothly up and down within a range of ±1 mm at 1 Hz. The average concentration of Eu^{2+} can be kept low, and hence the back-reaction to Eu^{3+} is suppressed.These experiments correspond to enlargement of the irradiation volume, therefore indicating that dilution will reduce the efficiency of the back reaction. The observed Eu^{2+} concentration was in fact more than 4 times higher than that expected from the simulated curve for a laser intensity of 0.5 mJ.

The efficiency, $\phi_{3\rightarrow 2}$, of Eu^{3+} to Eu^{2+} is defined as follows:

$$\phi_{3\rightarrow 2} = \frac{[Eu^{2+}]\ \text{observed}}{\text{calcd photons absorbed by } Eu^{3+}} \qquad (1)$$

The number of photons absorbed by Eu^{3+}, as indicated in the denominator of the above equation, is calculated based upon several assumptions. Single photon absorption is assumed. Then, although laser energy may also be absorbed by the Eu^{2+} ion, this phenomenon is neglected. Eu^{3+} has an absorption coefficient of $\epsilon_{3+} = 2.9\ M^{-1}\ cm^{-1}$ for the $^5L_6 \leftarrow {}^7F_0$ transition, although the spectral width of the laser pulse, 3.4 nm, is wider than the 2 nm of the transition. The calculated number of photons absorbed by Eu^{3+} in the vicinity of the surface is $Sn(2.303 \times 10^3)\epsilon_{3+}I_0[Eu^{3+}]/V = 6.2 \times 10^{-2}$ M, where I_0 is the photon number expressed with units of Einstein/cm^2 with 0.50 mJ per pulse and Sn is the number of irradiating laser shots. V is a factor of volume dilution, in this case, 76.3. The observed concentration was 5.2×10^{-3} M at 2000-shot irradiation. Therefore, $\phi_{3\rightarrow 2}$ (moving cell) $= 5.2 \times 10^{-3}$ M/6.2×10^{-2} M $= 0.084$, was estimated.

3.3. Multiphoton Reduction via $^5L_6$ Excitation. The observed Eu^{2+} concentrations after 10 000 laser shots, $[Eu^{2+}]^{obs}_{10000}$, are plotted in Figure 5. The apparent efficiencies were estimated to be 0.016 (0.79 mJ, 10 000 shots) and 0.0048

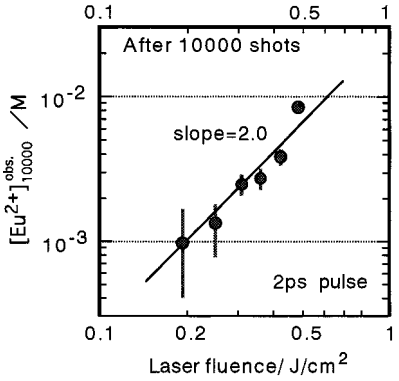

Figure 5. $[Eu^{2+}]^{obs}_{10000}$, the concentration after 10000 laser shots where Eu^{2+} has been averaged in the sample, are plotted vs laser fluence. The oblique solid line has a slope of 2.0. The vertical lines on the circles are reading errors.

(0.31 mJ, 10 000 shots). The Eu^{2+} concentrations are proportional to the square of the laser fluence. The reduction of Eu^{3+} to Eu^{2+} clearly proceeds via multiphoton processes, although these results include the back-reaction. In fact, the reduction can be explained by introducing a three-photon process, and the efficiency for the first shot reaches 0.3, as discussed later.

Figure 6 shows the excitation wavelength dependence. $[Eu^{2+}]^{obs}_{10000}$ at 0.50 mJ/pulse (●) are plotted vs the central wavelengths of the excitation pulse. It can clearly be seen that the conversion efficiency was high if the laser wavelength was tuned to the peak of the Eu^{3+} transition, $^5L_6$. Similar results were obtained by irradiation of 9600 shots with 0.015 mJ per pulse in 0.35 ps, where the maximum concentration of Eu^{2+} was 4×10^{-3} M and the other two values were normalized. On the basis of these observations, the reduction of Eu^{3+} to Eu^{2+} proceeds via the $^5L_6$ state.

4. Discussion

4.1. Saturation Behavior Explained by the Back Reaction. The reaction scheme is thought to be as follows:

$$Eu^{3+}X \xrightarrow{h\nu} (Eu^{3+})^*X \xrightarrow{h\nu}\xrightarrow{h\nu} (Eu^{2+}X^+)^* \rightsquigarrow Eu^{2+} + X^+$$

$$Eu^{2+}Y \xrightarrow{h\nu} (Eu^{2+}Y)^* \rightsquigarrow Eu^{3+} + Y^- \qquad (2)$$

The first photon at 394.3 nm pumps the f-electronic transition of $^5L_6 \leftarrow {}^7F_0$, and the second and the third photons pump into the CT states. X can be Cl^-, methanol, or H_2O. The final CT state efficiently dissociates to Eu^{2+}. The existence of a back-reaction is introduced to explain the saturation behavior of the photoproduct formation of Eu^{2+}. Y can be methanol or H_2O. The back-reaction is accompanied by H_2 production when Y = H_2O, as follows:

$$Y^- = HO^- + H^\bullet$$

$$H^\bullet + CH_3OH \rightarrow H_2 + {}^\bullet CH_2OH \qquad (3)$$

It should be noted that small bubbles assignable to H_2 production were observed during laser irradiation. The appreciable bubble formation can be seen when a solution containing Eu^{3+} is irradiated with an excimer laser at 308 nm under the intensities far below ablation threshold. Eu^{3+} is reduced to Eu^{2+} and the photo-back-reaction occurs. The intensity of the femtosecond laser is below the threshold of laser ablation. These observations support H_2 formation; however, the components of the bubbles were not analyzed.

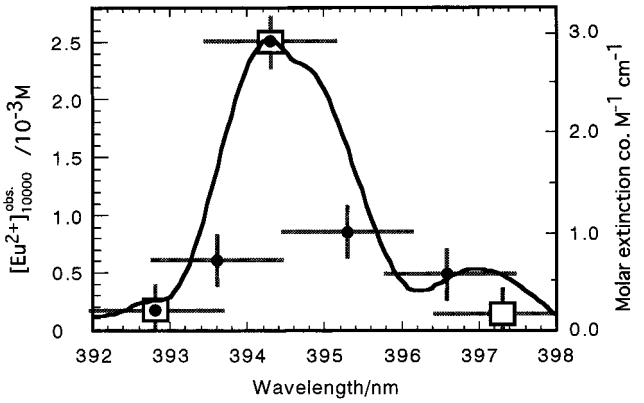

Figure 6. Wavelength dependence of the concentration of Eu^{2+} vs the laser central wavelength. Irradiation by 10000 shots with a 2 ps pulse width at 0.50 mJ/pulse (●) with the concentrations indicated by the vertical scale on the left. Irradiation by 9600 shots with a 0.35 ps pulse at 0.015 mJ/pulse (□); the maximum concentration was 4×10^{-3} M and the other two values are normalized. The vertical lines indicate error bars. The horizontal bars indicate the spectral half-width of the laser pulse. The solid curve is the absorption spectrum around the $^5L_6 \leftarrow {}^7F_0$ transitions with the molar extinction coefficients indicated by the vertical scale on the right.

Reaction scheme 2 is expressed by the following differential and integrated equations:

$$\frac{\Delta[Eu^{2+}]}{\Delta S} = \phi^1_{3\rightarrow 2} I_{3+}[Eu^{3+}] - \phi_{2\rightarrow 3} I_{2+}[Eu^{2+}] \quad (4)$$

$$[Eu^{2+}]^{calc}_{Sn} = \phi^1_{3\rightarrow 2} I_{3+}[Eu^{3+}] \frac{1 - \exp(-\phi_{2\rightarrow 3} I_{2+} Sn)}{\phi_{2\rightarrow 3} I_{2+}} \quad (5)$$

$\Delta[Eu^{2+}]$ is the rate of concentration increase by ΔS laser shots. $\phi^1_{3\rightarrow 2}$ is a special term referring to the conversion efficiency of the first shot from Eu^{3+} to Eu^{2+}. The second term in eq 4 is the back-reaction in response to the laser excitation of Eu^{2+}, where I_{2+} at the surface is $(2.303 \times 10^3)\epsilon_{2+} I_0$, $\epsilon_{2+} = 40$ M^{-1} cm^{-1}, and $\phi_{2\rightarrow 3}$ is the back-reaction quantum yield from Eu^{2+} to Eu^{3+}. The photooxidation of Eu^{2+} to Eu^{3+} has been known since 1948, and the reaction produces hydrogen.[15−17] Davis et al.[17] have measured the yields of hydrogen production ϕ_{H2} at several excitation wavelengths and have pointed out that twice the value of ϕ_{H2} is reasonably in agreement with the old values.[15,17] The $\phi_{2\rightarrow 3}$ value at the laser wavelength of 394.3 nm was interpolated to be 0.11 from the data by Davis et al.

The integration of eq 4 gives $[Eu^{2+}]^{calc}_{Sn}$ in eq 5 as a calculated concentration of Eu^{2+} after Sn laser shots. Sn is the number of the laser shots in the period of continuous irradiation. The back-reaction causes saturation effects, which can be seen in Figure 4. When Sn = 90, the quantity of Eu^{2+} produced is 90 times that of $\phi^1_{3\rightarrow 2} I_{3+}[Eu^{3+}]$, but 47.3% is expected to photochemically returns to Eu^{3+} according to eqs 4 and 5. The final $[Eu^{2+}]^{calc}_{90}$ value is evaluated to be 47.4 times that of $\phi^1_{3\rightarrow 2} I_{3+}[Eu^{3+}]$ using a $\phi_{2\rightarrow 3}$ value of 0.11 and 0.79 mJ /pulse irradiation. $[Eu^{2+}]^{calc}_{Sn}$ is calculated to approach a constant, when Sn > 500 in all power range in the present experiments. The constant simply means that $[Eu^{2+}]$ and $[Eu^{3+}]$ are in a photochemical equilibrium.

To draw the simulation curves as shown in Figure 4, the experimental procedure was taken into account. After the solution was irradiated for 1 s (10 shots), the Eu^{2+} fluorescence was measured to determine the concentration. The fluorescence measurement took about 10 min. The next cycle of irradiation and measurement took 10 s and 10 min, respectively. The last cycle was 500 s of irradiation and 10 min of fluorescence measurement. The back-reaction rate depends on the concentration of Eu^{2+} or, in other words, on the diffusional dilution of Eu^{2+}.

We have tried to create simulation curves to reproduce the experimental points in Figure 4 by applying eq 5, which does not include the effect of diffusional dilution. As a first approximation, the diffusional dilution is complete in 200 s, but no dilution occurs in less than 100 s. For the case of 10000-shot irradiation as an example, the Eu^{2+} concentration after 10 000 shots was calculated according to the irradiation procedure, as follows:

$$[Eu^{2+}]^{calc}_{10000} = [Eu^{2+}]^{calc}_{10} + [Eu^{2+}]^{calc}_{90} + [Eu^{2+}]^{calc}_{400} + [Eu^{2+}]^{calc}_{500} + [Eu^{2+}]^{calc}_{1000} + [Eu^{2+}]^{calc}_{3000} + [Eu^{2+}]^{calc}_{5000} \quad (6)$$

The 10 000 in the $[Eu^{2+}]^{calc}_{10000}$ on the left of eq 6 indicates the total number of laser shots. Each number of laser shots in the period of continuous irradiation at 10 Hz is shown in the subscript of each term on the right side of eq 6. An increase in the Eu^{2+} concentration was observed after 5000 laser shots. This increase is probably due to the diffusional dilution effect of the Eu^{2+} ion. To simulate the experimental results, either $[Eu^{2+}]^{calc}_{3000}$ or $[Eu^{2+}]^{calc}_{5000}$ was approximated to be twice the value of $[Eu^{2+}]^{calc}_{1000}$. The calculated values are drawn as broken lines in Figure 4. The simulation curves reproduce the experimental observations fairly well. Then, $\phi^1_{3\rightarrow 2}$ can be evaluated from the data after 10 000 shots and the fitted numerical values in the simulation curves.

We should first of all compare the experimental observation $\phi_{3\rightarrow 2}$ (moving cell) where the back-reaction is suppressed and a first shot efficiency $\phi^1_{3\rightarrow 2}$ where no back reaction occurs. The experimental observation value of 0.084 for $\phi_{3\rightarrow 2}$ (moving cell) and the 0.101 simulated value, $\phi^1_{3\rightarrow 2}$, at 0.50 mJ laser energy are satisfactorily close. The relationship of $\phi^1_{3\rightarrow 2} > \phi_{2\rightarrow 3}$ (moving cell) is reasonable. The highest efficiency was simulated to be 0.329 for $\phi^1_{3\rightarrow 2}$ at the highest irradiation energy of 0.79 mJ and these values are plotted on Figure 5.

The highest efficiency of the three-photon process is close to one-third, in other words, the photoreduction efficiency is close to unity for the third photon. The efficiency of geminate recombination from $Eu^{2+}X$ to Eu^{3+} X^- is suggested to be low. A similar low efficiency, namely, a high photoreduction efficiency, has been observed for the case of one-photon excitation to the CT band by a UV laser.[18] The one-photon efficiency is 0.97 ± 0.2 for a system of $EuCl_3$ in methanol on irradiation with a UV laser (308 nm).

4.2. Three-Photon Formation and One-Photon Back-Reaction. The reduction efficiency $\phi^1_{3\rightarrow 2}$ and the concentration of Eu^{2+}, $[Eu^{2+}]^{calc}_1$, in response to the first shot are extracted from the simulation curves based on eqs 4−6 and are plotted in Figure 7. An extracted concentration of $[Eu^{2+}]^{calc}_1$ is expected at the surface without diffusional dilution. The efficiency itself $\phi^1_{3\rightarrow 2}$ is found to be proportional to the square of the laser fluence. The $[Eu^{2+}]^{calc}_1$ is proportional to the cube of the laser fluence. The experimentally observed values of $[Eu^{2+}]^{obs}_{10000}$ in Figure 5 are proportional to the square of the laser fluence. The square relationship for $[Eu^{2+}]^{obs}_{10000}$ and the cube relationship for $[Eu^{2+}]^{calc}_1$ indicate that the reduction takes place as a three-photon process and that a one-photon back-reaction is included.

4.3. Initial Process of One-Photon Absorption by the $^5L_6$ State and Suppression of Multiphoton Ionization of Solvent.

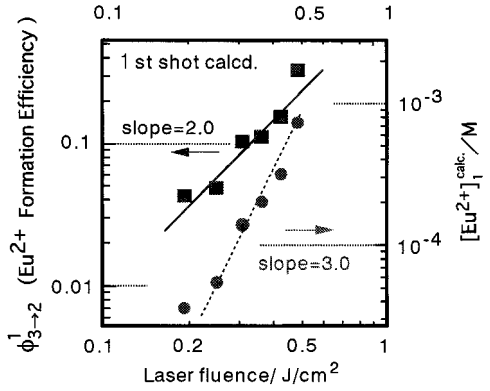

Figure 7. The calculated efficiency, $\phi^1_{3\to2}$ (■), and concentration, $[Eu^{2+}]^{calc}_1$, by the first shot (●) are plotted vs the laser fluence. The oblique, solid line and the dotted line have slopes of 2.0 and 3.0, repectively. $[Eu^{2+}]^{calc}_1$ is a calculated concentration at the position where the laser irradiated, with no diffusional dilution.

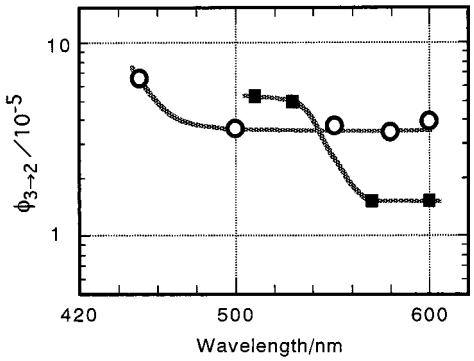

Figure 8. Eu^{2+} formation by nanosecond two-photon and two-color excitation. The first shot was fixed at 394.3 nm corresponding to the $^5L_6 \leftarrow {}^7F_0$ transition symbolized by a square (■). The open circles (○) indicate a fixed laser wavelength of 464.7 nm, which corresponds to the peak wavelength of the $^5D_2 \leftarrow {}^7F_0$ transition. The horizontal scale shows the wavelength of the second dye laser.

Solvated electrons can reduce Eu^{3+} to Eu^{2+}, as has been observed in the field of radiochemistry.[19,20] The reactions observed in the present experiments are not due to the multiphoton ionization of methanol. The multiphoton ionization of methanol should not show a wavelength dependence within a range of a few nanometers. The present irradiation energy was lower than 2.5×10^{11} W/cm^2 and can probably produce solvated electrons if pure methanol is used. Solvated electrons have been known to form from pure methanol using a 300 fs laser focusable to more than 10^{13} W/cm^2 at 620 nm.[21] Even from water, three-photon excitation is capable of forming solvated electrons with an irradiation energy of about 10^{11} W/cm^2 at 351 nm.[22] These reactions were studied using several laser lines in a wide range of wavelengths of 620−193 nm. Figure 6 clearly shows the excitation wavelength dependence within a range of a few nanometers. The photoprocess with the lowest threshold take places first. Our system includes Eu^{3+}, which can absorb photons by a one-photon process. This process obviously has the lowest threshold, and other multiphoton processes, including formation of solvated electron, are therefore suppressed.

It should be noted that clear wavelength dependencies have been observed by the present group by dye laser excitation with a pulse width of 20 ns.[4] This reduction occurs via two-step excitation, and one of the intermediates is the $^5L_6$ state. The mechanism for this reduction is rather similar to the case of Sm^{2+} oxidation to Sm^{3+} that has been observed by Winnacker et al.[3] Either $^5D_0 \leftarrow {}^7F_0$ or $^5D_1 \leftarrow {}^7F_0$ transitions of Sm^{2+} were excited with CW red dye laser lines, and the second green photon ionizes Sm^{2+} to Sm^{3+} + e. On the other hand, the multiphoton reduction of Eu^{3+} in a crystal of KBr has been reported in response to nanosecond dye laser excitation.[23] In the reported experiment, there was no clear relation between the excitation spectrum of the reduction and the absorption spectrum of Eu^{3+}. The excitation spectrum was monotonical and higher as it moved toward shorter wavelengths. They suggested that the reduction proceeds via quantum mechanical multiphoton processes.

There is another possibility of solvated electron formation. Electron may be ejected from the state pumped by the third photon. Some of the electrons can escape from the initial pair and could be trapped by an Eu^{3+} ion, and the reaction produces Eu^{2+}. The quantum yields of the escape probability are not very high for several inorganic monoions studied by laser excitation[24] and are in the range of 0.02 and 0.55. Consequently, the CT excitation mechanism is appropriate to explain the high reduction efficiency in the present experiments more than the electron ejection mechanism.

4.4. Higher CT Excitation Leads to a More Effective Reduction. Two-color and two-photon excitation by nanosecond lasers can enhance reduction efficiencies.[5] New data were obtained, and the new calibration line for the Eu^{2+} concentration was used in this study (Figure 8). The first photon was fixed at the transition $^5L_6 \leftarrow {}^7F_0$ (394.3 nm) with a laser fluence of 440 mJ/cm^2. The laser fluence of the second laser was kept at 490 mJ/cm^2. The efficiency was measured for the first photon irradiated. The efficiencies were measured at four different wavelengths.The 394.3 nm laser light itself induces two-photon reduction, and the efficiency was 1.5×10^{-5}. At two short wavelengths, 510 and 530 nm, the efficiencies were enhanced to 3.5 times that of conditions without the second photon. For the case of the first photon tuned to the $^5D_2 \leftarrow {}^7F_0$ (464.7 nm) transition, five wavelengths were examined for the second photon. The efficiency reached 7×10^{-5} at the shortest wavelength, 450 nm, and at other wavelengths were the same as that obtained without the second color. The two lasers were operated at the same time for the above experiments. No enhancement was observed when the second laser was delayed 50 ns. The lifetimes of the intermediates are shorter than 50 ns. The results directly indicate that neither $^5D_1$ nor $^5D_0$ can be an intermediate of the two-photon reduction because the two states have lifetimes that are much longer than microseconds.

When the total photon energy is higher than 5.4 eV (230 nm), the efficiency is enhanced based on the wavelength dependencies of the two-color and two-photon experiments. The CT band of $EuCl_3$ in methanol starts from 350 nm toward short wavelengths and the excitation to this band by one-photon excitation induces photoreduction with a high yield.[18] One of our important findings from this study is that the photoreactive CT band moves to the high-energy side from the f-electron excited states.

The short-pulse excitation described in the present paper succeeded in dramatically enhancing the photoreduction efficiency to 0.3 from 10^{-5} by nanosecond lasers. The dependency on the laser fluence indicates that there is a three-photon rather than a two-photon process for the case of nanosecond pulse excitation. Possible explanations for the efficient reduction are as follows. To reduce Eu^{2+} to Eu^{3+}, higher CT levels are more reactive. The higher state has a shorter lifetime, and a shorter laser pulse can therefore pump effectively from a CT state to higher CT levels. The lifetime of the CT level reached by the second photon of a nanosecond pulse is probably too short to be excited by the nanosecond lasers to the labile CT level. It is

quite natural that the charge separation and corresponding escape probability increases with excitation energy. This tendency is supported by reduction efficiencies of Eu^{3+} to Eu^{2+} by one-photon excitation to CT bands with deep UV lasers.[18] Higher efficiency is observed at shorter excitation wavelengths.

5. Conclusions and Possible Applications

Several features of this paper are summarized below.

(i) The excitation of an f-electronic excited state has been known to exhibit low reactivity; however, this paper has succeeded in demonstrating that an efficient photochemical reaction is induced via an f-electric excited state by an intense laser pulse. The efficiency of the multiphoton reduction of Eu^{3+} to Eu^{2+} in methanol is dramatically enhanced to 0.3 by short-pulse excitation compared with the 10^{-5} efficiency by nanosecond lasers.

(ii) The tunability of a Ti:sapphire laser can be effectively utilized to tune the laser wavelength to the transition of an f-electronic state, which has a narrow spectral width.

(iii) New questions arise based on the results presented here. Why cannot the $^5D_1$ or $^5D_0$ states with long lifetimes be intermediates? Why do active CT levels shift to the higher energy side if the f-electronic states are excited?

(iv) The photochemical reactions of lanthanide and actinide ions are expected to be utilized for nuclear fuel reprocessing.[25] Am is one of the key elements in the waste. The photoreaction of the Am ion has been observed.[26] Am has an electronic structure of $5f^57s^2$ and Eu $4f^76s^2$. Therefore, Am^{3+} may be responsive to multiphoton excitation as is Eu^{3+}. The $^5L_6$ level is located at 503.2 nm,[27] and multiphoton oxidation may be induced.

Acknowledgment. The authors thank Mr. Hiroki Ueyama and Mr. Tomoyuki Kuge for operating the femtosecond laser system. Financial support was provided in part by Kansai Electric Co. Ltd.

References and Notes

(1) Jørgensen, C. K. *Mol. Phys*. **1962**, *5*, 271. Jørgensen, C. K. In *Handbook on the Physics and Chemistry of Rare Earths*; Gschneidner, K. A., Jr., Eyring, L., Eds.; Elsevier: North-Holland, 1988; Vol. 11, Ch. 75; pp 197−292.

(2) Donohue, T. *Opt. Eng*. **1979**, *18*, 181.

(3) Winnacker, A.; Shelby, R. M.; Macfarlane, R. M. *Opt. Lett*. **1985**, *10*, 350.

(4) Kusaba, M.; Nakashima, N.; Izawa, Y.; Yamanaka, C.; Kawamura, K. *Chem. Phys. Lett.* **1994**, *221*, 407.

(5) Reported in part: Nakashima, N. *Rev. Laser Eng*. **1996**, *24*, 787; **1997**, *26*, 117 (both in Japanese).

(6) Nakashima, N.; Kusaba, M.; Izawa, Y.; Yamanaka, C.; Kawamura, W. *JAERI-CONF*, *95-005* **1995**, *2*, 891.

(7) Schillinger, H.; Sakabe, S.; Kuge, T.; Ueyama, H.; Urano, T.; Kawato, S.; Hashida, M.; Shimizu, K.; Kou, J.; Izawa, Y. *Rev. Laser Eng*. **1997**, *25*, 890.

(8) Cooley, R. A.; Yost, D. M. *Inorg. Synth*. **1946**, *2*, 69.

(9) Adachi, G.; Sorita, K.; Kawata, K.; Tomokiyo, K.; Shiokawa, J. *Inorg. Chim. Acta* **1985**, *109*, 117.

(10) Carnall, W. T.; Fields, P. R.; Rajnak, K. *J. Chem. Phys.* **1968**, *49*, 4450.

(11) Keller, B.; Bukietyńska, K.; Jeżowska-Trzebiatowska, B. *Bull. Acad. Pol. Sci. Ser. Sci. Chim*. **1976**, *24*, 763.

(12) Haas, Y.; Stein, G. *J. Phys.Chem.* **1971**, *75*, 3668.

(13) Sveshnikov, E. B.; Naumov, S. P. *Opt. Spectrosc*. **1978**, *44*, 72.

(14) Horrocks, W. DeW., Jr.; Albin, M. Lanthanide Ion Luminescence in Coordination Chemistry and Biochemistry. In *Progress in Inorganic Chemistry*; John Wiley & Sons: New York, 1984; pp 1−104.

(15) Brandys, M.; Stein, G. *J. Phys. Chem.* **1978**, *82*, 852.

(16) Douglas, D. L.; Yost, D. M. *J. Chem. Phys*. **1949**, *17*, 1345; **1950**, *18*, 1687.

(17) Davis, D. D.; Stevenson, K. L.; King, G. K. *Inorg. Chem.* **1977**, *16*, 670.

(18) Kusaba, M.; Nakashima, N.; Kawamura, W.; Izawa, Y.; Yamanaka, C. *Chem. Phys. Lett.* **1992**, *197*, 136; *J. Alloys Compd*. **1993**, *192*, 284.

(19) Ishida, A.; Takamuku, S. *Chem. Lett*. **1988**, *1988*, 1497.

(20) Selin, D. L.; Tarasova, N. P.; Malkov, A. V.; Poskrebyshev, G. A. *React. Kinet. Catal. Lett.* **1989**, *39*, 273.

(21) Pépin, C.; Goulet, T.; Houde, D.; Jay-Gerin, J.-P. *J. Phys. Chem.* **1994**, *98*, 7009.

(22) Crowell, R. A.; Bartels, D. M. *J. Phys. Chem.* **1996**, *100*, 17940.

(23) Yamada, Y.; Ohno, S. *Chem. Lett*. **1991**, *1991*, 465.

(24) Iwata, A.; Nakashima, N.; Kusaba, M.; Izawa, Y.; Yamanaka, C. *Chem. Phys. Lett.* **1993**, *207*, 137.

(25) Donohue, T. *Chemical and Biochemical Applications of Lasers*; Moore, C. B., Ed.; Academic Press: New York, 1980; Vol. 5, pp 239−273.

(26) Yussov, A. B.; Shilov, V. P. *Radiokhim.* **1993**, *35*, 38 (in Russian).

(27) Katz, J. J.; Seaborg, G. T.; Morss, L. R. *The Chemistry of the Actinides Elements*, 2nd ed.; Chapmann and Hall: New York, 1986.